ACS APPLIED MATERIALS & INTERFACES

Research Article

www.acsami.org

Hard Carbon Originated from Polyvinyl Chloride Nanofibers As High-Performance Anode Material for Na-Ion Battery

Ying Bai,[†] Zhen Wang,[†] Chuan Wu,[†] Rui Xu,[‡] Feng Wu,*[,†] Yuanchang Liu,[†] Hui Li,[†] Yu Li,[†] Jun Lu,*[,‡] and Khalil Amine*[,‡]

[†]Beijing Key Laboratory of Environmental Science and Engineering, School of Chemical Engineering annd Environment, Beijing Institute of Technology, Beijing 100081, China

[‡]Chemical Sciences and Engineering Division, Argonne National Laboratory, Lemont, Illinois 60439, United States

ABSTRACT: Two types of hard carbon materials were synthesized through direct pyrolysis of commercial polyvinyl chloride (PVC) particles and pyrolysis of PVC nanofibers at 600−800 °C, respectively, where the nanofibers were prepared by an electrospinning PVC precursors method. These as-prepared hard carbon samples were used as anode materials for Na-ion batteries. The hard carbon obtained from PVC nanofibers achieved a high reversible capacity of 271 mAh/g and an initial Coulombic efficiency of 69.9%, which were much superior to the one from commercial PVC, namely, a reversible capacity of 206 mAh/g and an initial Coulombic efficiency of 60.9%. In addition, the hard carbon originated from the PVC nanofibers exhibited good cycling stability and rate performance: the initial discharge capacities were 389, 228, 194, 178, 147 mAh/g at the current density of 12, 24, 60, 120, and 240 mA/g, respectively, retaining 211 mAh/g after 150 cycles. Such excellent cycle performance, high reversible capacity, and good rate capability enabled this hard carbon to be a promising candidate as anode material for Na-ion battery application.

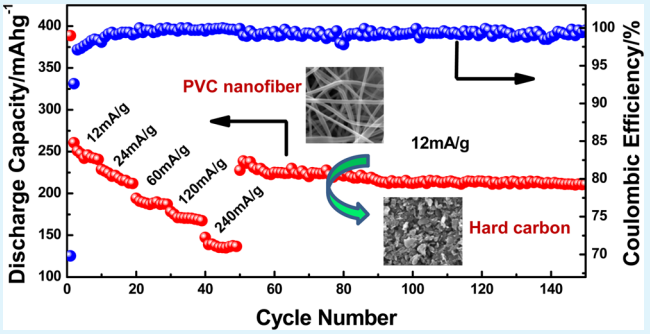

KEYWORDS: *Na-ion battery, hard carbon, polyvinyl chloride nanofiber, electrospinning*

1. INTRODUCTION

Alongside the development of Li-ion battery, Na-ion battery was initially studied in the late 1970s. However, the further application of lithium-based technology to mass storage systems faces inevitable challenges in terms of both lithium resources and the cost.[1] In recent years, Na-ion battery has drawn much interest as a power source for large-scale grid energy storage, because of the advantages in abundance and low cost.[2] In the same main group, sodium behaves the similar physical and chemical properties as lithium,[5] but is found much more abundant in nature on the earth. As an inexhaustible and unlimited resource,[3] it is commonly existing in seawater and constituting 2.8% by mass of the earth's crust.[4] Therefore, benefiting from low cost, long cycle life, and room-temperature operation, Na-ion battery has been proposed as a promising candidate for application in large-scale energy storage system.[6]

Because the diameter of Na^+ is 0.106 nm, which is about 55% bigger than that of Li^+ (0.076 nm), a good Na-insertion electrode material must have sufficiently large interlayer space within their crystallographic structure to host Na^+ ions.[5−7] Recently, a few anode materials have been found with large open tunnels to accommodate Na^+.[1] However, most of them exhibit low capacity, poor reversibility and electronic conductivity, or high volume expansion accompanying Na^+ insertion−extraction reaction. The petroleum-coke carbon[8] showed low reversible capacity of 80 mAh/g at 86 °C; the NASICON structure $NaTi_2(PO_4)_3$[9] can only bring a capacity of 85 mAh/g, though with a theoretical value of 133 mAh/g; the metal-oxide material TiO_2 nanotube[10] only can remains 150 mAh/g within 15 cycles; the organic compound $Na_2C_8H_4O_4$[11] has to combine a lot of conducting materials like Ketjen black (as high as 20%) because of its poor electronic conductivity; the alloyed nanocomposite SnSb/C,[12] expanded its volumes to 400% during charge and discharge, leading to low initial Coulombic efficiency and poor cyclic stability.

Recently, hard carbon materials, such as pyrolytic carbon with glucose precursor,[13] PAN-based carbon fibers,[14] and carbon microspheres,[15] have attracted more attention because of their large interlayer distance and disordered structure, which are beneficial for Na^+ insertion−extraction. Komaba et al.[3] reported that a hard carbon is capable of exhibiting a reversible capacity of 240 mAh/g at a rate of 25 mA/g, but its high rate performances were not discussed. Also by using hard carbon, the good initial reversible capacities of 300 and 285 mAh/g were obtained by Stevens[13] and Alcántara et al.,[15] respectively, but the cyclabilities were not satisfied. In contrast, some other studies reported hard carbons performed rather good cyclability of over 100 cycles, but low specific capacities less than 250

Received: January 28, 2015
Accepted: February 18, 2015
Published: February 18, 2015

DOI: 10.1021/acsami.5b00861
ACS Appl. Mater. Interfaces 2015, 7, 5598−5604

Scheme 1. Schematic Diagram of Synthesis Routes and Na^+ Storage Behaviors of Hard Carbon Samples As Anode Materials for Na-Ion Batteries: (a) Hard Carbon Originated from PVC Nanofibers, (b) Hard Carbon Originated from PVC Particles

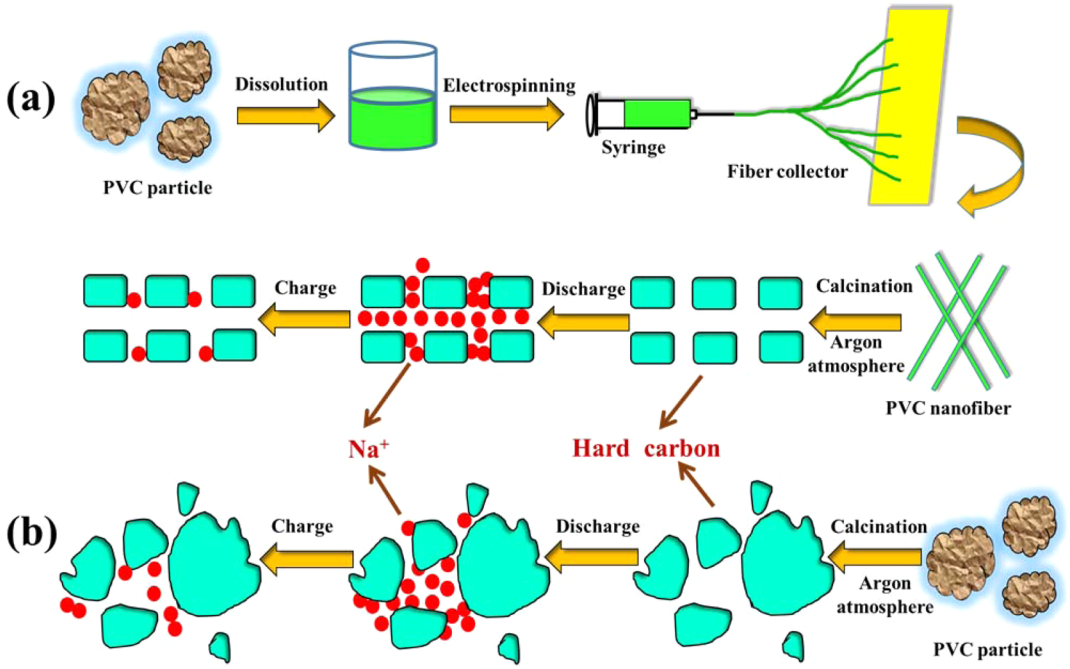

mAh/g.[3] Nevertheless, Cao et al.[16] prepared hollow carbon nanowires through pyrolyzation of self-assembly hollow polyaniline nanowires precursor, and successfully achieved a reversible capacity of 251 mAh/g as well as excellent cycling stability. Such results also proved that, fabricated from self-assembly precursors, nanofiber, or nanowire carbon was able to work as better anode materials behaving excellent electrochemical properties. In fact, there are many other methods can also efficiently fabricate nanofibers or nanowires, such as electrospinning[6,17] or template synthesis.[18]

In this paper, we prepared high-performance hard carbon from pyrolyzing PVC nanofibers, which were fabricated by using electrospinning method. For comparison, commercial PVC particle was selected as another precursor to produce reference hard carbon. The electrochemical characteristics of these two types of as-prepared samples for Na-ion battery anodes were evaluated and discussed.

2. EXPERIMENTAL SECTION

Synthesis of Hard Carbon Samples. Polyvinyl chloride (PVC) purchased from Aladdin with a molecular mass of 500 was used as received, while tetrahydrofuran (AR) and dimethylformamide (AR) (volume ratio = 3.5:6.5) were mixed as a cosolvent. The schematic diagram of different hard carbon samples synthesis routes is shown in Scheme 1. Certain amount of PVC was dissolved in the cosolvent with stirring until the solution became a transparent viscous liquid.[19] The concentration of the as-prepared PVC precursor solution is 15 w/V%. Then electrospinning was carried out at an applied voltage of 17 kV. The PVC solution was fed at a constant rate of 0.05 mm/min. The collection distance between the needle tip and the collector was 12 cm. Then the precursors were calcined with the heating rates of 5 °C/min at 0−200 and 1 °C/min above 200 °C. Argon was used as a protective gas running through the tube furnace at a flow rate of 200 cm^3/min, as illustrated in Scheme 1a). As listed in Table 1, the hard carbon samples (EP-600, 700, 800) were synthesized from the pyrolysis of the electrospun PVC (EP) at 600, 700, and 800 °C, respectively. For comparison, the reference hard carbon sample (CP-700) was produced from direct pyrolysis of commercial PVC (CP) particles at 700 °C, as illustrated in Scheme 1b).

Table 1. (002) Diffraction Peaks of Different Hard Carbon Samples

sample	precursor	pyrolysis temperature (°C)	2θ (deg)	d_{002} (nm)
EP-600	PVC nanofibers	600	25.31	0.3516
EP-700	PVC nanofibers	700	25.39	0.3505
EP-800	PVC nanofibers	800	25.41	0.3502
CP-700	PVC particles	700	25.56	0.3481

Characterization of the As-Prepared Samples. The crystalline structures of the hard carbon samples were characterized by a Rigaku DMAX2400 X-ray diffractometer with Cu−Kα radiations in the 2θ range 10° to 80°. The scan rate was 8°/min in step of 0.02°. The morphologies of the samples were observed by a JSM-35C scanning electron microscope.

Electrochemical Tests. The as-prepared hard carbon samples were crushed into uniform powders. The slurry was prepared by mixing hard carbon powder with 10 wt % acetylene black, and 10 wt % of a solution containing 10 wt % polyvinylidene fluoride (PVDF) binder dissolved in *N*-methylpyrrolidinone (NMP). Then, the slurry was coated on a copper foil collector and followed by a vacuum drying at 80 °C for 24 h to remove the residual NMP solvent, the loading of hard carbon on the electrode is around 1.5 mg/cm^2. The coin cells were assembled in an argon atmosphere glovebox (MBRAUN-6020). A mixture of 1 M $NaPF_6$ in ethylene carbonate (EC) and diethyl carbonate (DEC) (1:1 by volume) was prepared as electrolyte. A sodium foil was chose as counter electrode. A commercial Celgard 2400 membrane was used as the separator. The charge−discharge performances were evaluated by a LAND-CT2011A battery tester at a constant current density of 12 mA/g. Cyclic voltammograms were recorded on a CHI608E electrochemical workstation. The scan rate was 0.1 mv/s.

3. RESULTS AND DISCUSSION

To understand the suitable calcining temperatures for PVC pyrolysis, we recorded the thermal properties of PVC by

DOI: 10.1021/acsami.5b00861
ACS Appl. Mater. Interfaces 2015, 7, 5598−5604

thermogravimetric (TG) analysis. As shown in Figure 1, it is clear that there are two thermal decomposition stages for PVC.

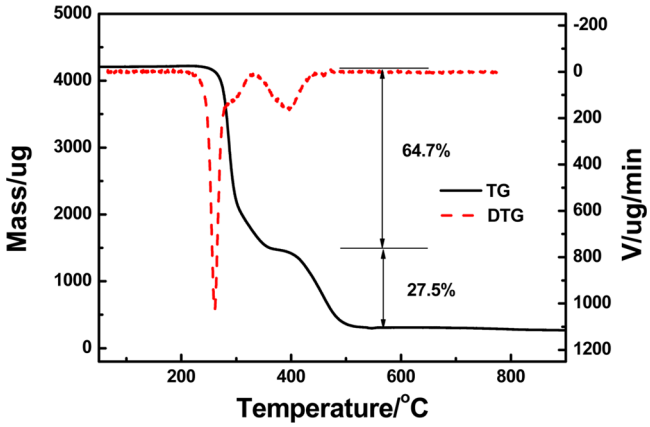

Figure 1. TG-DTG profiles of commercial PVC.

The first one is from 250 to 380 °C with a weight loss of 64.7 wt %, which can be attributed to a rapid removal of HCl. The second one is from 410 to 520 °C with a weight loss of 27.5 wt %, which is considered to be a restructuring process, such as the elimination of remaining Cl, aromatization and chain cross-linking. From Figure 1, the pyrolysis should be completed only when the temperature is higher than 520 °C without any further mass loss. Therefore, 600, 700, and 800 °C were selected as different calcination temperatures to obtain optimized microstructures of hard carbon materials.

The XRD patterns of different hard carbon samples are shown in Figure 2. All of the curves are correspond to the

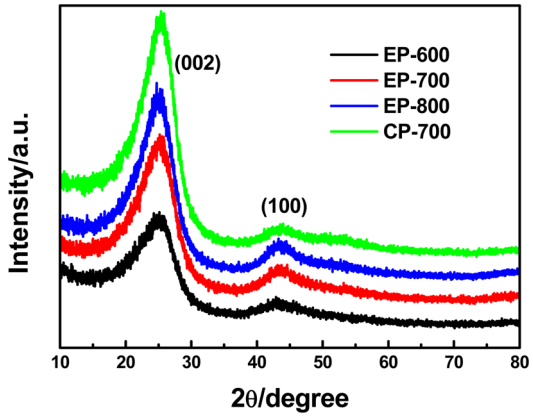

Figure 2. XRD patterns of different hard carbon samples originated from PVC nanofibers or PVC particles.

(002) and (100) diffractions of the hard carbon. It is worth noting that, with the increasing temperature, the diffraction peak (002) of EP moves to higher angle with increased intensity. It is also found that the higher temperature helps to form the better crystallization and the smaller carbon interlayer space (Table 1). From the 2θ degree of the (002) peak, the value of interlayer distance (d_{002}) is calculated to be larger than the one of graphite (0.335 nm). Such larger interlayer space allows Na^+ insertion to happen more easily. Additionally, it indicates that the morphology of PVC precursor is the key factor affecting the *d*-space during the synthesis, because all the hard carbon samples originated form PVC nanofibers have larger *d*-space than the one originated form PVC particles.

As shown in Figure 3a, the as-spun PVC nanofibers possess smooth surface and uniform diameter (about 100 nm), which is

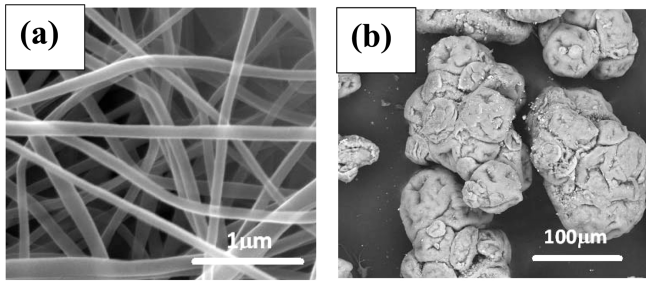

Figure 3. SEM images of the PVC precursors. (a) PVC nanofibers prepared by electrospinning, (b) commercial PVC particles.

~1000 times smaller than that of commercial PVC (Figure 3b). Figure 4a–d present the apparent morphology of the hard carbon materials originated from different synthesis route and calcined at various temperatures. Comparing with EP-600 and EP-800, EP-700 has a more uniform particle distribution while showing smaller particle size. Meanwhile, a disparity of the particle sizes has been found in CP-700. Also, some large massy particles with rough surface are formed, on which many surface-attached small particles are observed.

Each sample's laser diffraction particle size analysis follows a unimodal distribution. EP-600 shows a peak of the distribution at around 1.9 μm and all particles are sized less than 6.6 μm. EP-700 has a most common size value around 850 nm and all of its particles are smaller than 2.5 μm. The particle size distribution rang (−10 μm) of EP-800 is the widest among the EP samples, which is mostly distributed around 2.5 μm. As for sample CP-700, the particle size is determined mainly around 3.9 μm in a range of 0−15 μm. All the data above are consistent with the SEM observations results, namely, have the same variation tendency. Thus, it is expected that the small particle size of EP-700 is suitable to enlarge the contact area between electrode and electrolyte, and shorten the diffusion path lengths for Na^+,[18,20,21] predicting the improvement potentials of electrochemical performance.

The Na^+ storage behaviors of the hard carbon samples are concluded in Figure 5. The irreversible capacity in all first cycles is caused by the electrolyte decomposition and the solid electrolyte interphase (SEI) formation. In Figure 5a, when the PVC nanofiber precursor was calcined at 600 °C, the as-obtained hard carbon shows its lowest reversible capacity, only 214 mAh/g, among all of the samples. Such low capacity is due to its incomplete carbonization,[22] as described by the weak (002) diffraction intensity in Figure 2. As the temperature increases to 700 °C, the hard carbon EP-700 achieves better graphitization, more uniform morphology, differences among micropores and more interaction of sodium with heteroelements[14,15,20] (e.g., H or O). Consequently, its sodium storage property was greatly improved associating with promising initial discharge and reversible capacity of 389 and 271 mAh/g, respectively. As the temperature is further reached to 800 °C, the carbon interlayer space becomes smaller (Figure 2) and brings difficulties for Na^+ insertion/exaction in EP-800, leading to the lower initial charge and discharge capacities. Hence, the calcined temperature is crucial to the Na^+ storage properties and electrochemistry performance.

DOI: 10.1021/acsami.5b00861
ACS Appl. Mater. Interfaces 2015, 7, 5598−5604

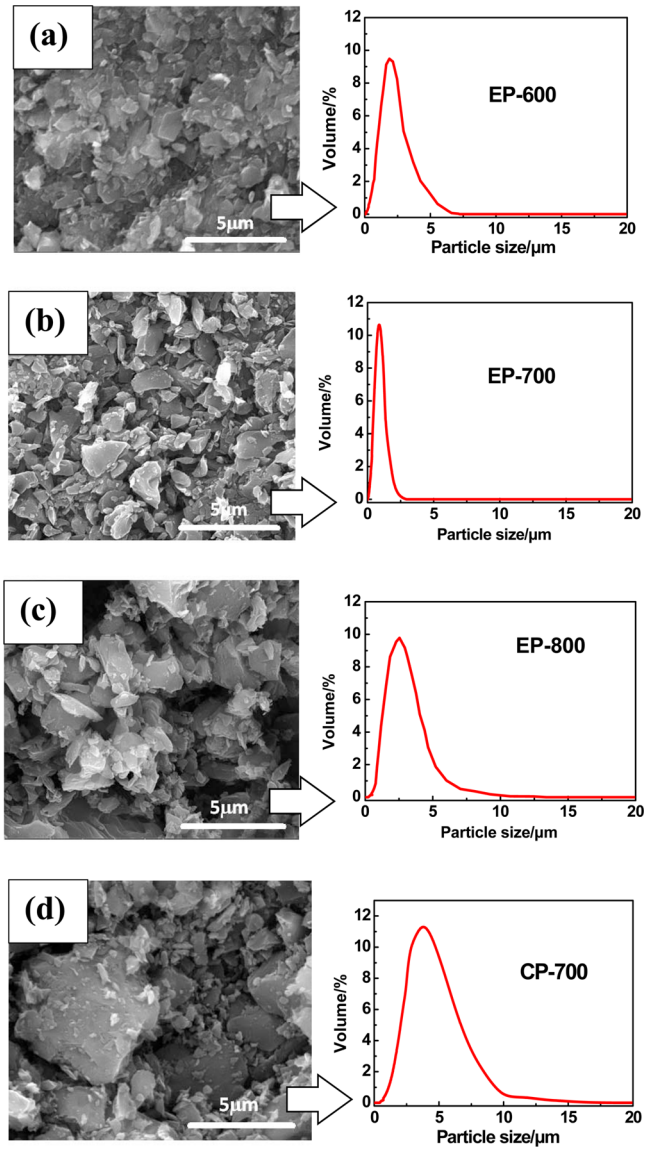

Figure 4. SEM images of the raw PVC materials and as-prepared samples. (a) EP-600, (b) EP-700, (c) EP-800, (d) CP-700. For the as-prepared samples, the right-hand represents the corresponding particle distribution.

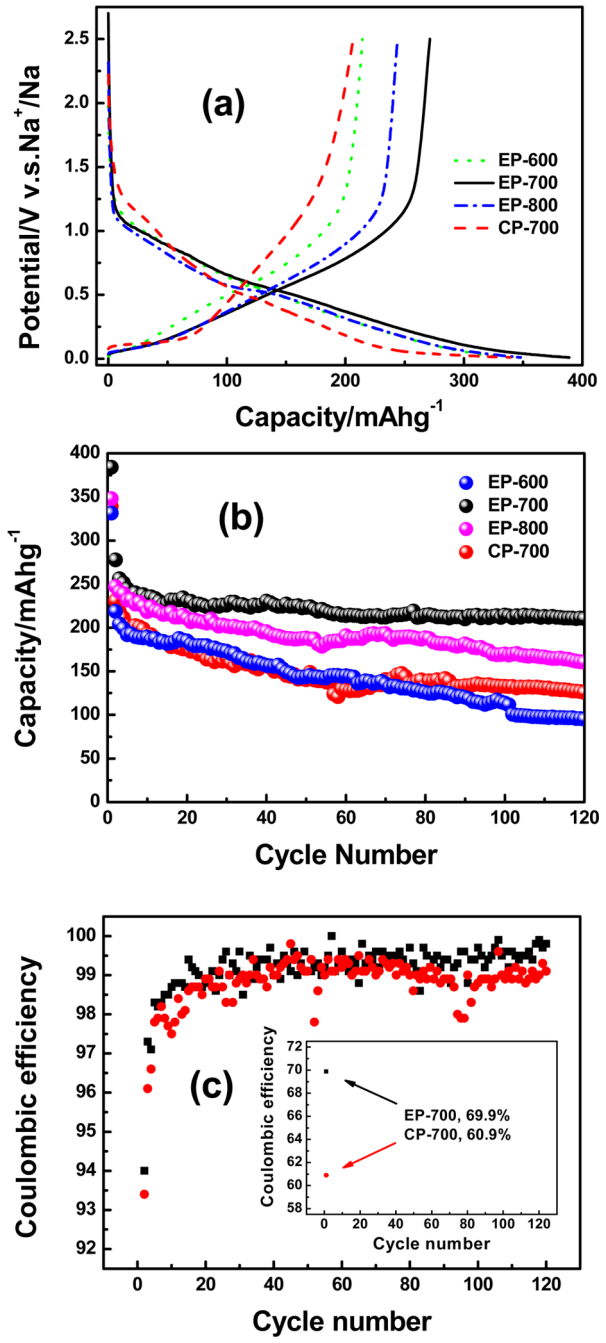

Figure 5. Electrochemical evaluation of the hard carbon materials originated from PVC fibers or particles. (a) Initial discharge−charge profiles for EP and CP hard carbon samples. (b) Cycling performance of EP and CP electrodes tested at 12 mA/g, the voltage range is between 0.01 and 2.5 V. (c) Coulombic efficiencies of EP-700 and CP-700 upon cycling.

Obviously, when compared with the one originated from the PVC particles, EP-700 has better charge and discharge capacities than CP-700, as shown in Figure 5a. The reasons why EP-700 exhibits such a better charge/discharge capacity can be ascribed to several following aspects: first, the lager interlayer distance of EP-700 allowed an easier and faster insertion/extraction process in its host materials. Also, EP-700 was made of smaller particles with larger contact area between electrode and electrolyte, as well as shorter distance of Na^+ intercalation and deintercalation.[16,21] Thus, it was able to accelerate the charge transfer between the interfaces,[10] and improve the discharge capacity and coulomb efficiency. Furthermore, the sodium insertion mechanism is intercalation between the interlayers, insertion into the porosity of the host structure, adsorption on single layers, and reactions with heteroelements.[23] As a result, the defects in its host structure are reduced, which improves the performance and stability.

The cycling testing at a constant current density of 12 mA/g (Figure 5b and Table 2) confirms that the electrochemical performances are enhanced by the prosperous nanocrystallization of electronspun PVC precursor calcined at 700 °C. Directly fabricated from PVC particles, CP-700 exhibits an initial discharge capacity of only 339 mAh/g, followed by a quick decrease to 218 mAh/g after 3 cycles, and remains at 126 mAh/g after 120 cycles because of a heavy capacity loss. On the other hand, EP-700 originated from PVC nanofibers shows much superior electrochemical performances: an initial

DOI: 10.1021/acsami.5b00861
ACS Appl. Mater. Interfaces 2015, 7, 5598−5604

Table 2. Discharge Specific Capacities of the Hard Carbon Samples Originated from PVC Nanofibers or PVC Particles

	discharge capacity at various cycles (mAh/g)		
sample	first	third	120th
EP-600	331	204	95
EP-700	389	256	211
EP-800	348	241	161
CP-700	339	218	126

discharge capacity of 389 mAh/g, a reversible discharge capacity of 256 mAh/g at the third cycle, and a discharge capacity of 211 mAh/g for 120 cycles. However, although EP-600 also originates from PVC precursor nanofibers, it offers initial capacities of 331 mAh/g and 95 mAh/g after 50 cycles, which are relatively lower than the other three samples. Because the heating temperature of EP-600 is not high enough, this sample shows an incomplete carbonization structure, which is not in favor of good reversible Na^+ transfer, and results in inferior electrochemical performances. It is consistent with the results of initial discharge−charge profiles, proving again that the post-processing temperature has crucial effects on the nanocrystallization and battery performances. In addition, for the well-carbonized hard carbon samples EP-700, EP-800, and CP-700, the sample with smaller particle size distribution showed better electrochemical performance, because small particle size distribution can help enlarging the surface area (better contact with the electrolytes) and shortening the Na^+ diffusion distance.

Furthermore, it is notable that both of the hard carbon materials originating from PVC nanofibers or particles have satisfactory Coulombic efficiencies, as shown in Figure 5c. Samples EP-700 and CP-700 have initial Coulombic efficiencies of 69.9 and 60.9%, respectively, which can be observed in the inset of Figure 5c. In the second cycle, the Coulombic efficiencies of EP-700 and CP-700 remarkably increase to 94 and 93.4%, respectively. This implies that the formation of solid electrolyte interphase (SEI), along with possible side reactions, is mainly accomplished in the initial cycle. After that, the Coulombic efficiencies of the two hard carbons achieve around 99% in the subsequent cycles. At the 120th cycle, very high Coulombic efficiencies are still remained, namely, 99.8% for EP-700 and 99.1% for CP-700. This phenomenon is very attractive, because it indicates that the hard carbon materials from PVC pyrolysis are promising anode candidates for Na-ion batteries. Furthermore, the average Coulombic efficiencies (from 11th to 120th) are 99.3% for EP-700 and 98.9% for CP-700, which signifies EP-700 originated from PVC nanofibers has superior electrochemical stability upon cycling.

The Na^+ insertion−extraction behaviors of hard carbon from different routes were further investigated by cyclic voltammetry. For EP-700 in Figure 6a, a pair of redox peaks appears within 1.0 V, corresponding to the insertion and extraction process of Na^+. In addition, the disappeared peaks at 0.35 and 0.39 V in the subsequent cycles reveal an irreversible capacity in the initial cycle. Such phenomenon of capacity loss in the initial cycle is likely originated from the concomitant formation of SEI associated with the decomposition of the electrolyte,[11,18,24] which is consistent with Figure 5b and Table 2. The well-overlapped CV curves in the subsequent cycles are indicating that the SEI formations mainly have accomplished during the initial cycle, which are in accord with the results in Figure 5c. Subsequently, the electrode displays an excellent stability of

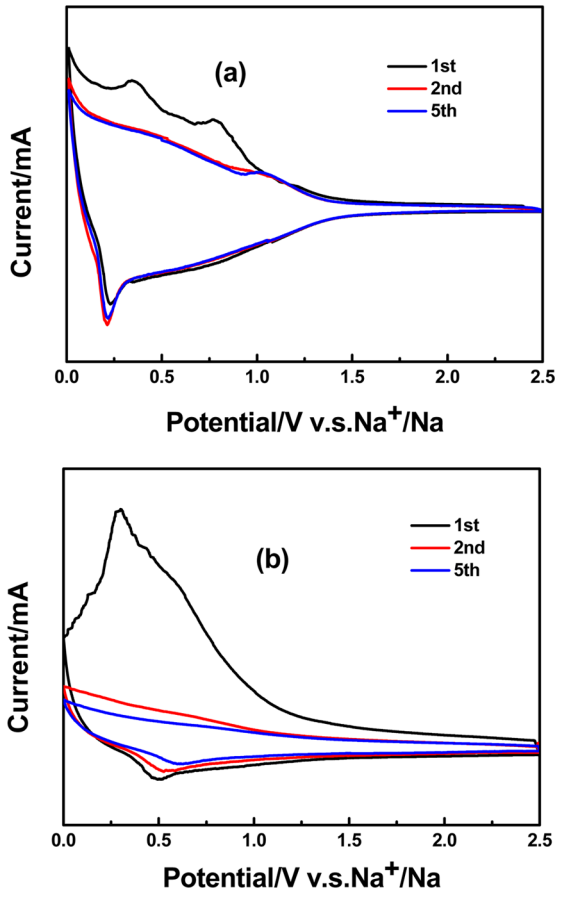

Figure 6. Cyclic voltammogram curves of (a) EP-700 and (b) CP-700 at a scan rate of 0.1 mV/s between 0.01 and 2.5 V.

Na^+ insertion-extraction in the following cycles. The low-potential plateaus of the hard carbon material can be attributed to the insertion of Na^+ into the nanopores between randomly stacked layers through a process analogous to adsorption.[11,13] This process make the Na^+ likely to be inserted into the sites with chemical potential close to that of sodium, thus giving a potential value of ~0 V.[20,25,26] It is found that the side-reaction of CP-700 in the initial cycle is much more evident than EP-700, as shown in Figure 6b. The extremely strong peak between 0 and 1.2 V disappears in the subsequent cycles, indicating the significant capacity loss happens in the initial cycle, which is consistent with the cycling performance shown in Figure 5.

Apparently, EP-700, the one originated from PVC nanofibers and calcined at 700 °C, showed the best electrochemical performances. To further evaluate the rate performances, sample EP-700 was cycled at the current rates of 12, 24, 60, 120, and 240 mA/g, and achieves an initial discharge capacity of 389, 228, 194, 178, 147 mAh/g, respectively, as shown in Figure 7. Moreover, cycling at a high current density did not permanently damage the structure of its electrode. The high capacity can be recovered when the rate reduced as low as 12 mA/g. For long-term cycling, a constant discharge capacity of 211 mAh/g is well kept after 150 cycles at the current of 12 mA/g. The Coulombic efficiency afterward stays near 100%. The results demonstrate that the hard carbon originated from PVC nanofibers also exhibits excellent high rate capability and structural stability.

In Figure 7, the evolution of the Coulombic efficiency at various current densities is very similar to that at the low

DOI: 10.1021/acsami.5b00861
ACS Appl. Mater. Interfaces 2015, 7, 5598−5604

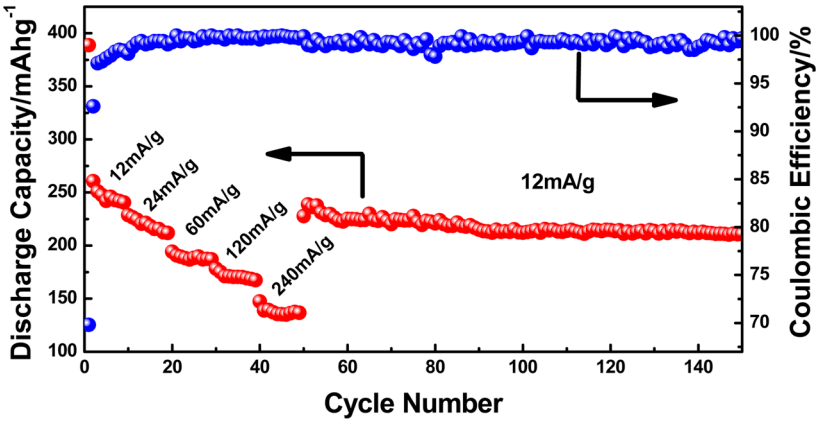

Figure 7. Discharge capacities and Coulombic efficiencies of EP-700 at different current densities of 12, 24, 60, 120, and 240 mA/g, respectively.

current density in Figure 5b. In addition, it is found that the increasing current densities will not deteriorate the Coulombic efficiency of EP-700. Namely, the Coulombic efficiencies at the 20th, 30th, 40th and 50th cycles, which are corresponding to the last cycles at the current densities of 24, 60, 120, and 240 mA/g, are 99.3, 99.8, 99.6, and 99.9%, respectively. It means that high current density can only cause polarization, but will not intensify the side reactions.

4. CONCLUSIONS

In summary, hard carbon EP-600, 700, and 800 were successfully prepared through pyrolysis of PVC nanofibers, which originated from electrospinning. When used as anode materials for Na-ion batteries, EP-700 showed the most excellent electrochemical performance among all samples. That is, the hard carbon electrode can achieve an initial reversible capacity of 271 mAh/g and retain 215 mAh/g after 120 cycles at 12 mA/g. Even at a high current density of 240 mA/g, the electrode still can reach a reversible capacity of 147 mAh/g, and a Coulombic efficiency of 99.9%. The results showed that such hard carbon electrode was behaving excellent cyclability, high rate capability, high Coulombic efficiency and structural stability. For comparison, the electrode of CP-700, which originated from PVC particles, recovered a reversible capacity of only 206 mAh/g, accompanied by a quick decrease to 126 mAh/g. Thus, the EP-700 hard carbon is a promising anode electrode material for Na-ion batteries. The outstanding electrochemical performance can be attributed to its moderate graphitization, larger interlayer distance, and small particle size. Besides, hard carbons prepared from the various types of precursors and temperatures were performing different electrochemical properties. Furthermore, for the well-carbonized hard carbon samples heated at 700 °C or higher temperatures, the sample with smaller particle size distribution showed better electrochemical performance, because small particle size distribution can help achieving better contact between the electrode and the electrolyte, and shortening the Na^+ diffusion distance. Therefore, choosing a proper carbon source, a suitable fabrication condition, and an appropriate method to modify the structure is crucial to achieve desired materials for Na-ion batteries.

AUTHOR INFORMATION

Corresponding Authors

*E-mail: wufeng863@bit.edu.cn.
*E-mail: junlu@anl.gov.
*E-mail: amine@anl.gov.

Notes

The authors declare no competing financial interest.

ACKNOWLEDGMENTS

This work is supported by National Basic Research Program of China (Grant No. 2015CB251100), Program for New Century Excellent Talents in University (Grant NCET-13-0033), and Beijing Higher Institution Engineering Research Center of Power Battery and Chemical Energy Materials. Argonne National Laboratory is operated for the U.S. Department of Energy by UChicago Argonne, LLC, under contract DE-AC02-06CH11357. Y.B. acknowledges the support from the State Scholarship Fund (201406035025) of the China Scholarship Council.

REFERENCES

(1) Li, H.; Wu, C.; Wu, F.; Bai, Y. Sodium Ion Battery: A Promising Energy-Storage Candidate for Supporting Renewable Electricity. *Acta Chim. Sin.* **2013**, *72*, 21−29.
(2) Slater, M. D.; Kim, D.; Lee, E.; Johnson, C. S. Sodium-Ion Batteries. *Adv. Funct. Mater.* **2013**, *23*, 947−958.
(3) Komaba, S.; Murata, W.; Ishikawa, T.; Yabuuchi, N.; Ozeki, T.; Nakayama, T.; Ogata, A.; Gotoh, K.; Fujiwara, K. Electrochemical Na Insertion and Solid Electrolyte Interphase for Hard-Carbon Electrodes and Application to Na-Ion Batteries. *Adv. Funct. Mater.* **2011**, *21*, 3859−3867.
(4) Dunn, B.; Kamath, H.; Tarascon, J.-M. Electrical Energy Storage for the Grid: A Battery of Choices. *Science* **2011**, *334*, 928−935.
(5) Palomares, V.; Serras, P.; Villaluenga, I.; Hueso, K. B.; Carretero-González, J.; Rojo, T. Na-Ion Batteries, Recent Advances and Present Challenges to Become Low Cost Energy Storage Systems. *Energy Environ. Sci.* **2012**, *5*, 5884−5901.
(6) Li, H.; Bai, Y.; Wu, F.; Li, Y.; Wu, C. Budding Willow Branches Shaped $Na_3V_2(PO_4)_3$/C Nanofibers Synthesized Via an Electrospinning Technique and Used as Cathode Material for Sodium Ion Batteries. *J. Power Source* **2015**, *273*, 784−792.
(7) Chevrier, V.; Ceder, G. Challenges for Na-Ion Negative Electrodes. *J. Electrochem. Soc.* **2011**, *158*, A1011−A1014.
(8) Doeff, M. M.; Ma, Y.; Visco, S. J.; De Jonghe, L. C. Electrochemical Insertion of Sodium into Carbon. *J. Electrochem. Soc.* **1993**, *140*, L169−L170.
(9) Wu, W.; Mohamed, A.; Whitacre, J. Microwave Synthesized $NaTi_2(PO_4)_3$ as an Aqueous Sodium-Ion Negative Electrode. *J. Electrochem. Soc.* **2013**, *160*, A497−A504.
(10) Xiong, H.; Slater, M. D.; Balasubramanian, M.; Johnson, C. S.; Rajh, T. Amorphous TiO_2 Nanotube Anode for Rechargeable Sodium Ion Batteries. *J. Phys. Chem. Lett.* **2011**, *2*, 2560−2565.

DOI: 10.1021/acsami.5b00861
ACS Appl. Mater. Interfaces 2015, 7, 5598−5604

(11) Zhao, L.; Zhao, J.; Hu, Y. S.; Li, H.; Zhou, Z.; Armand, M.; Chen, L. Disodium Terephthalate ($Na_2C_8H_4O_4$) as High Performance Anode Material for Low-Cost Room-Temperature Sodium-Ion Battery. *Adv. Energy Mater.* **2012**, *2*, 962−965.
(12) Xiao, L.; Cao, Y.; Xiao, J.; Wang, W.; Kovarik, L.; Nie, Z.; Liu, J. High Capacity, Reversible Alloying Reactions in SnSb/C Nanocomposites for Na-Ion Battery Applications. *Chem. Commun.* **2012**, *48*, 3321−3323.
(13) Stevens, D.; Dahn, J. High Capacity Anode Materials for Rechargeable Sodium-Ion Batteries. *J. Electrochem. Soc.* **2000**, *147*, 1271−1273.
(14) Thomas, P.; Billaud, D. Electrochemical Insertion of Sodium into Hard Carbons. *Electrochim. Acta* **2002**, *47*, 3303−3307.
(15) Alcántara, R.; Lavela, P.; Ortiz, G. F.; Tirado, J. L. Carbon Microspheres Obtained from Resorcinol-Formaldehyde as High-Capacity Electrodes for Sodium-Ion Batteries. *Electrochem. Solid State Lett.* **2005**, *8*, A222−A225.
(16) Cao, Y.; Xiao, L.; Sushko, M. L.; Wang, W.; Schwenzer, B.; Xiao, J.; Nie, Z.; Saraf, L. V.; Yang, Z.; Liu, J. Sodium Ion Insertion in Hollow Carbon Nanowires for Battery Applications. *Nano Lett.* **2012**, *12*, 3783−3787.
(17) Bae, H.; Lee, J. Encapsulated Particles Attached on Electrospun Fibers by In Situ Combination of Electrospinning and Coaxial Electrospraying. *J. Nanosci. Nanotechno.* **2014**, *14*, 7574−7580.
(18) Wenzel, S.; Hara, T.; Janek, J.; Adelhelm, P. Room-Temperature Sodium-Ion Batteries: Improving the Rate Capability of Carbon Anode Materials by Templating Strategies. *Energy Environ. Sci.* **2011**, *4*, 3342−3345.
(19) Lee, K. H.; Kim, H. Y.; La, Y. M.; Lee, D. R.; Sung, N. H. Influence of a Mixing Solvent with Tetrahydrofuran and N, N-Dimethylformamide on Electrospun Poly (vinyl chloride) Nonwoven Mats. *J. Polym. Sci., Polym. Phys.* **2002**, *40*, 2259−2268.
(20) Thomas, P.; Billaud, D. Effect of Mechanical Grinding of Pitch-Based Carbon Fibers and Graphite on Their Electrochemical Sodium Insertion Properties. *Electrochim. Acta* **2000**, *46*, 39−47.
(21) Miao, Y.-E.; Fan, W.; Chen, D.; Liu, T. High-Performance Supercapacitors Based on Hollow Polyaniline Nanofibers by Electrospinning. *ACS. Appl. Mater. Interfaces* **2013**, *5*, 4423−4428.
(22) Sun, Y.-K.; Lee, K.-H.; Moon, S.-I.; Oh, I.-H. Effect of Crystallinity on the Electrochemical Behaviour of Spinel $Li_{1.03}Mn_2O_4$ Cathode Materials. *Solid State Ionics* **1998**, *112*, 237−243.
(23) Gotoh, K.; Ishikawa, T.; Shimadzu, S.; Yabuuchi, N.; Komaba, S.; Takeda, K.; Goto, A.; Deguchi, K.; Ohki, S.; Hashi, K. NMR Study for Electrochemically Inserted Na in Hard Carbon Electrode of Sodium Ion Battery. *J. Power Sources* **2013**, *225*, 137−140.
(24) Cao, Y.; Xiao, L.; Wang, W.; Choi, D.; Nie, Z.; Yu, J.; Saraf, L. V.; Yang, Z.; Liu, J. Reversible Sodium Ion Insertion in Single Crystalline Manganese Oxide Nanowires with Long Cycle Life. *Adv. Mater.* **2011**, *23*, 3155−3160.
(25) Thomas, P.; Billaud, D. Sodium Electrochemical Insertion Mechanisms in Various Carbon Fibres. *Electrochim. Acta* **2001**, *46*, 3359−3366.
(26) Mochida, I.; Ku, C.-H.; Korai, Y. Anodic Performance and Insertion Mechanism of Hard Carbons Prepared from Synthetic Isotropic Pitches. *Carbon* **2001**, *39*, 399−410.

DOI: 10.1021/acsami.5b00861
ACS Appl. Mater. Interfaces 2015, 7, 5598−5604